Type B mandibuloacral dysplasia with congenital myopathy due to homozygous ZMPSTE24 missense mutation

Rabah Ben Yaou, Claire L. Navarro, Susana Quijano-Roy, Anne T. Bertrand, Catherine Massart, Annachiara de Sandre-Giovannoli, Juan Cadiñanos, Kamel Mamchaoui, Gillian S. Butler-Browne, Brigitte Estournet, et al.

Type B mandibuloacral dysplasia with congenital myopathy due to homozygous *ZMPSTE24* missense mutation.

Rabah Ben Yaou[1,2,3*], Claire Navarro[4*], Susana Quijano-Roy[1,2,5], Anne T. Bertrand[1,2], Catherine Massart[1,2], Annachiara De Sandre-Giovannoli[4], Juan Cadiñanos[6§], Kamel Mamchaoui[1,2], Gillian Butler-Browne[1,2], Brigitte Estournet[5], Pascale Richard[7], Annie Barois[5], Nicolas Levy[4,8], Gisèle Bonne[1,2,7]

* Equal contribution

1- Inserm, UMRS_974, Paris, France.

2- Université Pierre et Marie Curie- Paris 6, UM 76, CNRS, UMR 7215, Institut de Myologie, IFR14, Paris, France.

3- Association Institut de Myologie (AIM), GH Pitié-Salpêtrière, Paris, France.

4- Université de la Méditerranée - Inserm, UMR_S910, Génétique Médicale et Génomique Fonctionnelle, Faculté de Médecine de Marseille, Marseille, France.

5- AP-HP, Hôpital Raymond Poincaré, Service de Neuropédiatrie, Garches, France.

6- Departamento de Bioquímica y Biología Molecular. Universidad de Oviedo, Oviedo, Spain.

7- AP-HP, Groupe Hospitalier Pitié-Salpêtrière, U.F. Cardiogénétique et Myogénétique, Service de Biochimie Métabolique, Paris, France.

8- AP-HM, Département de Génétique Médicale – Hôpital d'enfants Timone, Marseille, France.

§ Current address: Instituto de Medicina Oncológica y Molecular de Asturias, Oviedo, Spain.

Author to whom correspondence and reprint requests are to be sent:

Gisèle Bonne, Inserm U974, Institut de Myologie, GH Pitié-Salpêtrière, 47 boulevard de l'Hôpital, 75651 Paris cedex 13, France. Tel: +33 1 42 16 57 23, Fax: +33 1 42 16 57 00, e-mail: g.bonne@institut-myologie.org

Running title: MADB with congenital myopathy

ABSTRACT

Mutation in *ZMPSTE24* gene, encoding a major metalloprotease, leads to defective prelamin A processing and causes type B mandibulo-acral dysplasia as well as the lethal neonatal restrictive dermopathy syndrome. Phenotype severity is correlated with the residual enzyme activity of ZMPSTE24 and accumulation prelamin A. We had previously demonstrated that a complete loss of function in ZMPSTE24 was lethal in the neonatal period whereas, compound heterozygous mutations including one PTC and one missense mutation were associated with type B mandibulo-acral dysplasia. Here, **we** report on a 30 year longitudinal clinical survey of a patient harboring a novel severe and complex phenotype, combining an early onset progeroid syndrome and a congenital myopathy with fibre type disproportion. A unique homozygous missense *ZMPSTE24* mutation (c.281T>C, p.Leu94Pro) was identified and predicted to produce 2 possible ZMPSTE24 conformations, leading to a partial loss of function. Western blot analysis revealed a major reduction of ZMPSTE24 together with the presence of unprocessed prelamin A and decreased levels of lamin A in the patient's primary skin fibroblasts. These cells exhibited significant reductions in lifespan associated with major abnormalities of the nuclear shape and structure. This is the first report of MAD presenting with confirmed myopathic abnormalities associated to ZMPSTE24 defects, extending the clinical spectrum of *ZMPSTE24* gene mutations. Moreover, our results suggest that defective prelamin A processing affects muscle regeneration and development thus providing new insights into disease mechanism of Prelamin A defective associated syndromes in general.

Keywords: ZMPSTE24, Mandibuloacral dysplasia, Congenital myopathy, prelamin A, Secondary laminopathies.

INTRODUCTION

ZMPSTE24 (also known as *FACE-1*) encodes a ubiquitously expressed zinc metalloprotease. Prelamin A, the lamin A precursor, is the only known substrate of ZMPSTE24 in mammals.[1] ZMPSTE24 is involved in post-translational proteolytic cleavage of carboxy terminal residues of farnesylated prelamin A to form mature lamin A.[2] Prelamin A is initially farnesylated on the last cystein within the prenylation "CaaX" motif at the C-terminus end of the protein, by a farnesyl-transferase.[3] Then, ZMPSTE24 or RCE1[4] removes the last three residues "aaX", before a carboxy-methyl group is added by the methyl transferase ICMT on the last remaining cystein.[5] Finally, a second cleavage is specifically performed by ZMPSTE24, removing the last 15 amino acids.[6] The product of this post-translational maturation pathway, mature lamin A, is located both at the nuclear lamina and the nucleoplasm. A-type lamins A and C, are expressed in all vertebrate differentiated cells, and are translated from alternatively spliced transcripts of the *LMNA* gene. After post-translational modifications A-type lamins assemble with B-type lamins to form the nuclear lamina, a filamentous meshwork underlying the inner nuclear membrane.[7]

While *LMNA* mutations are known to cause several phenotypes named "laminopathies" (OMIM *150330) involving striated muscles, adipose, nervous, cutaneous tissues and bone in isolated or combined fashions,[7,8] the responsibility of *ZMPSTE24* gene mutations (OMIM *606480) in human disease has been also recognized. By a candidate gene strategy resulting from phenotype similarities, various homozygous or compound heterozygous *ZMPSTE24* mutations were identified in two different and extremely rare premature ageing disorders: restrictive dermopathy (RD, OMIM #275210) and B type mandibuloacral dysplasia (MADB, OMIM #608612).[9-11] RD, the most severe disorder, is a lethal neonatal genodermatosis[12] characterized by intrauterine growth retardation, tight, rigid and easily eroded skin with prominent superficial vessels, bone mineralization defects, dysplastic clavicles, arthrogryposis and early neonatal death. MADB, an autosomal recessive disorder, characterized by skeletal abnormalities including mandible and clavicle hypoplasia, acro-osteolysis of the terminal

phalanges, mottled pigmentation, cutaneous atrophy and generalized lipodystrophy with metabolic syndrome such as insulin resistance, glucose intolerance, diabetes mellitus and hypertriglyceridemia.[13] In both disorders, no skeletal muscle involvement was reported so far.

The lack of ZMPSTE24 protein or its activity in cell lines from *ZMPSTE24* mutated patients resulted in misshapen nuclei containing abnormally aggregated lamin A/C associated with accumulation of unprocessed prelamin A.[10,11,14-16] Whereas the *ZMPSTE24* mutations found in MADB encoded a protein with considerable reduced residual activity, the mutations found in RD led to null ZMPSTE24 activity strongly suggesting a positive correlation between residual enzyme activity, accumulated prelamin A levels and the severity of the phenotype.[17] In *Zmpste24* knockout mice, severe growth retardation, skeletal abnormalities including small mandible, lipodystrophy, cardiomyopathy, muscular dystrophy were reported as well as premature death, these features being associated to a complete absence of mature lamin A and an exclusive production of prelamin A.[18,19] More importantly, several studies have demonstrated that blocking prelamin A farnesylation using either farnesyl transferase inhibitors (FTI) or a combination of statins and aminobisphosphonates could prevent prelamin A accumulation, extend longevity and ameliorate disease phenotype in *Zmpste24*$^{-/-}$ mice[4,20] leading to therapeutic trials in diseases associated to defective prelamin A processing.

Here, we report a 30 year longitudinal follow up of a patient carrying a new homozygous missense *ZMPSTE24* mutation leading to partial loss of enzymatic activity. The resulting clinical phenotype goes beyond the expected progeroid features and includes skeletal muscle involvement, suggesting that defective prelamin A processing may also induce muscle disease.

PATIENTS AND METHODS

Patient clinical history was assembled from the detailed medical reports of the neuropediatric department, Raymond Poincarré hospital, Assistance Publique Hôpitaux de

Paris (AP-HP), Garches, France, where the patient was followed along her whole life. Our study complies with the ethical guidelines of all the institutions involved.

Genetic analysis were performed on DNA samples from peripheral blood lymphocytes of the patient, her non affected parents, two sisters and one brother after informed consent. *LMNA* and *ZMPSTE24* gene screening was performed as described previously.[10,21] Confirmation of *ZMPSTE24* mutation (c.281T>C) was performed by enzymatic digestion of the PCR product using *Bsl*I (Ozyme, Saint-Quentin-en-Yvelines, France). *ZMPSTE24* conformations were predicted *in silico* using the two algorithms TMPred (http://www.ch.embnet.org/software/TMPREDform.hml) and TMHMM (http://www.cbs.dtu.dk/services/TMHMM-2.0/).

Primary skin fibroblasts were obtained from cultured skin biopsies of the patient and a normal control subject according to Muchir *et al*.[22]

Western blot analysis was performed from 40µg of protein homogenates on 10% SDS-PAGE for both control and patient primary skin fibroblasts. Detection of ZMPSTE24 and lamins A and C was performed using monoclonal anti-ZMPSTE24 antibody (205-8C10, Daiichi Chemical)[11] and polyclonal anti-lamin A/C antibody (H-110, Santa Cruz Biotechnologies, CA, USA).[21]

Immuno-fluorescence analysis of lamins A/C or prelamin A were then performed using polyclonal anti-lamin A/C (both at 1/100, Santa Cruz Biotechnologies) and FITC-conjugated anti-rabbit (1/500, Santa Cruz Biotechnologies) or Alexa-568 anti-goat (1/500, Invitrogen, USA) while emerin was detected by monoclonal MANEM5 anti-emerin (1/50, from G. Morris, NEWI, UK) and Alexa-568 anti-mouse (1/500, Invitrogen, USA).

Life span analysis of fibroblasts from the patient and an age-matched healthy control was performed as previously described.[23] Cell populations were serially passaged until they stopped dividing. At cell isolation, all cell populations were considered to be at 1 mean population doubling (MPD). The number of population doublings at every passage was

calculated as log (N/n)/log 2 where N is the number of cells at the time of passage divided by the number of cells initially seeded (n).

RESULTS

Clinical phenotype

The patient is the 4th female born to second degree related Portuguese parents. There were no other antecedents in the family. Hydramnios was detected intra-utero and delivery was premature at 35 weeks of gestational age. Birth weight was 1.715 kg (-3 SD), length 45 cm (-4 SD) and head circumference of 29.5 cm (-4SD) indicating intrauterine growth retardation. Apgar test was normal but two episodes of cyanosis were noted during the 1st day of life. Joint contractures were observed, including ankles, knees (popliteal angle=90°), hips and elbows. Skin was dysmature, with atrophic, dried, crumpled, and desquamated hyperkeratotic aspect. Dysmorphic features with retrognathia were also associated. Karyotype was normal. Polycythemia (hematocrit=63.1%) and thrombocytosis (thrombocyte count=514000/mm3) were also present at birth. Although mild axial and limb hypotonia was noted by the age of 3 months (mo), motor milestones were within normal ranges. She walked independently at 17mo. Difficulties to walk, climb stairs or rise from the floor appeared by the age of 2 years (y). Electromyography revealed myopathic patterns on deltoid, flexor carpi radialis and tibialis anterior muscles without spontaneous activities. Nerve conduction velocities were normal. Muscle weakness predominant in peri-scapular regions and proximal lower limbs progressed particularly from the age of 4y. There was scapular winging (figure 1, $a_{3\text{-}5}$). A deltoid muscle biopsy performed at 9y revealed myopathic changes suggestive of fibre type disproportion. There was fibre size variation with a large number of small fibres and type I fibre predominance (figure 1, d_1). All features were suggestive of a congenital myopathy with fibre type disproportion. In the second decade, muscle deficit spread to the 4 limbs. At 26y muscle weakness extended rapidly to distal lower limbs and electromyography examination

revealed peroneal nerve involvement in addition to a myopathic pattern at needle electromyography.

The patient demonstrated a severe failure to thrive (figure 1a), that led to a 'harmonic' dwarfism (figure 1, a_{1-5}). Varied and severe complications were observed during the course of the disease involving bones, skin, joints, skeletal, respiratory and cardiac muscles, and vascular, renal and hormonal systems. However, cognition was normal, she attended school, drove an adapted car and worked as an accountant until 25y.

Bone involvement was an early complication. Hypoplasia of the mandibula (figure 1, c_1), and left clavicle (figure 1,b_{1-4}) were detected by 5mo. Enlarged anterior fontanel, delayed skull ossification and tooth eruption (figure 1, c_2) were noted at 9mo, but after 4y teeth rapidly crowded (figure 1, c_3). Other bone abnormalities included femoral head dysplasia, and osteolysis, delayed bone maturation and distal finger osteolysis (figure 1, c_{5-6}). Long bones had characteristic enlarged metaphysis and slender diaphysis (figure 1, c_5). Decreased spine and limb bone density was associated with multiple spontaneous fractures, first observed in a clavicle at 6y (figure 1, b_{5-6}), and later in ribs, vertebrae and femur (figure 1, b_7). At 13y, osteolysis of the 3rd and 4th cervical vertebral spine process accompanied by C3-C4 and C7-D1 anterolisthesis occurred (figure 1, b_8). Cranial sutures were still open at 15y (figure 1, c_7). Serum calcium, phosphate and alkaline phosphatase levels were normal since birth.

Cutaneous abnormalities typical of progeria such as reduced subcutaneous fat were noted since birth. Generalized sclerodermic skin and abdominal papules were observed during the first year (figure 1, a_2). By 14mo, frontal and abdominal veins were dilated (figure 1, a_3) and the abdominal papules became beige and translucent. Later, blue spots appeared on the face and legs and a skin biopsy performed at 9y revealed sclerodermic features in the absence of deposits or inflammatory infiltrates. There was extreme dermal fibrosis, increased and often horizontally oriented elastic fibres, basal lamina horizontalisation and rare dermal papules (data not shown). Subcutaneous calcifications appeared in different sites (inter-phalangian

joints, cervical, dorsal and thoracic, figure 1, $c_{8\text{-}9}$). From 13.5y there was a rapid loss of hair evolving to alopecia in the year after (figure 1, a_6).

The cervical paravertebral calcifications caused spine and chest rigidity and other cervical subcutaneous nodules probably were responsible for swallowing difficulties observed at 15y. By 26y loss of muscle strength was predominant in lower limbs and a vertebral CT scan identified multiple subcutaneous and paravertebral calcifications at the cervicothoracic levels, infiltrating the left C7-T1 intervertebral foramen, the ribs and pushing back the scapula. Later, vertebral MRI and CT-scan revealed 2 intracanalar calcifications, one reducing medullar cavity diameter and another causing medullar compression and infiltrated the intervertebral foramen. Surgical ablation of these calcifications led to good functional recovery. Joint contractures associated with the short clavicles resulted in chest flatness with protuberant right chondro-costal joints. Joint mobility became very limited during the course of the disease at the ankles, knees and hips and a marked limitation of the mobility of shoulders and contractures of pectoral muscles was observed. With respect to the spine, by 2y a mild dorsal kypho-scoliosis was noted and associated cervical and lumbar lordosis due to axial weakness. A Milwaukee brace was indicated at 6y. By 15.5y, a dorsal gibbus was reported.

Respiratory complications were a late event but the patient died as a consequence of them. At 8y, diurnal hypersomnia, dyspnea, nocturnal snoring and an impressive laryngeal stridor prompted the first respiratory evaluation. Forced vital capacity (FVC) was reduced to 40% of theoretical value, with a significant fall in supine FVC with respect to sitting position, indicating a selective diaphragmatic failure and a major respiratory difficulty when lying. Polysomnographic evaluation revealed nocturnal apneas and marked desaturation. The patient was treated by non invasive noctural ventilation. Theophylline was also started. Restrictive respiratory insufficiency was observed (FVC of 37% at 10y and 28.2% at 25y).

ECG and echocardiography were normal until 24y when sinusal tachycardia, sharpened T waves, right bundle branch block, ventricular extrasystols and concentric left ventricular hypertrophy as well as high blood pressure were observed. At 27y, blood renin (34.9 pg/ml,

N<19) and aldosterone (207 pg/ml, N<125) were elevated concomitantly with hypokalaemia (3.3 mmol/l, N>3.5). This prompted a CT-scan of the renal arteries as well as MRI coupled with angiography and revealed bilateral calcifications of the renal arteries (figure 1, d_2) resulting in a 50% reduction in diameter without renal parenchyma vascularisation abnormalities. Atheromatous aortic infiltration was also observed (figure 1, d_3). High blood pressure was treated by acebutolol and enalapril with no significant improvement.

At 29y, chronic kidney disease with severe anaemia appeared and worsened progressively. Non-insulin dependent diabetes mellitus was diagnosed but no treatment was administered. The last evaluation at 30y showed elevated serum urea (23 mmol/l, N<7.5), creatinine (455 µmol/l, N<120) and phosphate (2.73 mmol/l, N<1.5) levels, the glomerular filtration rate was 9 ml/mn/1.73m^2 (N>80), proteinuria (6.9 g/l), glycosuria (2.5 g/l) and beta2 microglobinuria (25000 mg/24h). MAG3 scan revealed a global reduction in tracer uptake and excretion; all suggestive of multifactor chronic kidney disease with glomerular, vascular and tubular abnormalities. Due to bilateral renal artery calcifications, a revascularization procedure was suggested. Meanwhile, haemodialysis as well as chronic peritoneal dialysis were also considered. Subsequently, at 30 years of age, in this context of severe renal insufficiency and high blood pressure, the patient developed a lung infection. During this episode; she felt unwell, went to bed and was found dead in her bed at home. No autopsy was performed.

Further investigations have been performed. Blood testing revealed additional abnormalities during the disease. At 17mo, pre-betalipoproteins were slightly elevated (6.2 g/L, N<6). At 12y slight hearing loss was suspected at school. However, audiogram and auditory evoked potentials remained normal. Puberty was acquired at 12.5 y without menarche or menstrual period anomalies. The patient had poor breast development. Hormonal evaluation at 13y, revealed reduced dehydroepiandrosterone (1.6 ng/ml, N>2) and estradiol (27pg/ml, N>60), elevated somatostatin (28 pg/ml, N<10), with the remaining hormonal parameters remaining normal (cortisol, deoxycortisols, progesterone, androstenedione,

testosterone, corticotropin and prolactin). At 26.5y, hypertriglyceridemia (3.65 mmol/l, N<1.69) hypercholesterolemia (7.54 mmol/l, N<5.2) hypertransaminemia (ALAT: 201 IU/L, N<35; AST: 93 IU/L, N<34) and increased gamma-GT (244 IU/L, N<28) was observed. Abdominal ultrasonography revealed global hepatomegaly with steatosis with normal and symmetric ovaries. Medical treatment with simvastatin was started. CK were always within the normal range.

Genetic analysis

Because the main clinical features suggested a progeroid syndrome, with clinical features similar to MAD or HGPS, *LMNA* was first sequenced at the genomic level but no mutation was found in the exons or intron/exon boundaries. The *ZMPSTE24* gene was subsequently sequenced and a homozygous variation (c.281T>C) in exon 3, predicted to result in p.Leu94Pro was identified (figure 2a). This variation creates a new *Bsl*I restriction site that was further used to confirm the mutation in the patient and analyse its segregation within the family. A heterozygous c.281T>C variation was identified in the non affected parents, one sister and the brother, while it was absent in the other sister (figure 2b). This variation was not detected in more than 200 control chromosomes from unrelated subjects. Partial alignment of the ZMPSTE24 protein sequences from various species showed that the mutated Leucine 94 is highly conserved, suggesting an important role of this residue in the enzymatic activity (figure 2c). *In silico* predictions using TMHMM and TMpred programs, with either normal or mutated ZMPSTE24 protein sequences as matrix, indicated two possible conformational models: one corresponded to the normally folded protein including its seven consensus transmembrane (TM) domains, whereas the other lacked the second TM (figure 2d). Consequently this misfolded ZMPSTE24 predicted both its catalytic and endoplasmic reticulum (ER) signal mislocated in the ER lumen instead of cytoplasm, suggesting a loss of function or a mislocalisation. These predictions could not be considered as being mutually exclusive.

Western blot analysis

To determine whether or not these *ZMPSTE24* variations modify the expression of ZMPSTE24 protein, and consequently to prelamin A processing defects, western blot analyses were carried out on proteins extracted from the patient's cultured skin fibroblasts at passage P2. Immunoblots on the patient's fibroblast revealed an important decrease in the level of ZMPSTE24 compared to age matched control fibroblasts. As expected, this reduction was associated with the accumulation of prelamin A: in addition to the wild-type lamins A and C, an extra-band with higher molecular weight at the expected prelamin A size was observed (figure 2e). This supplementary band was absent from control fibroblasts also analysed at passage P2.

Life span and expression of prelamin A, lamin A/C and emerin of fibroblasts

The patient's fibroblasts were highly variable in size with a majority of the cells being larger than control cells. They tended to grow as clusters (figure 3) and exhibited a reduced life span (figure 4). Primary patient fibroblasts arrest their growth after only 56 days in culture (7 divisions). This is in contrast to primary control fibroblasts which made 38 divisions after 130 days in culture (figure 4). Patient fibroblasts exhibited major nuclear shape defects. Although lamins A/C and emerin were still localised at the nuclear rim together with prelamin A in all patient's fibroblasts, severe nuclear shape defects (lobulations, herniations) were observed, as compared with the uniform oval or round nuclei in the wild-type cells (figure 3).

DISCUSSION

This is the first report describing a MADB phenotype associated to myopathic features caused by a homozygous missense *ZMPSTE24* mutation. The pathogenicity of this unreported mutation was demonstrated by the presence of both prelamin A in protein extracts from patient fibroblasts, the abnormal shape of the fibroblast nuclei and the reduced lifespan of these fibroblasts.

In the literature, 30 patients carrying *ZMPSTE24* mutations have already been reported and have a large clinical spectrum going from typical RD to MADB. Apart from one,[24] the 23 patients with typical RD features had either homozygous or compound heterozygous null mutations (nonsense, insertions or deletions)[10,11,17,25-30] or very large in-frame deletions sometimes resulting from splice site mutations[10,11,16] in the *ZMPSTE24* gene. Moreover, all RD related mutations lead to a complete absence of the ZMPSTE24 protein or to null activity, consequently causing the accumulation of prelamin A and an absence of mature lamin A.[11,16,25] Two patients carrying *ZMPSTE24* mutations had progeroid features of variable severity. The first one, carrying compound nonsense and missense mutations, had been diagnosed as a severe progeroid phenotype and died at 2y.[14] The second one, carried a homozygous *ZMPSTE24* frameshift deletion associated to a *LMNA* heterozygous nonsense mutation which "rescued" the patient's phenotype, most probably by reducing to half the amounts of accumulated prelamin A, as in the double knock out *Zmpste24*$^{-/-}$ *Lmna*$^{+/-}$ mice.[15,31] This patient showed features compatible with a severe form of MADB, but was described as being affected with HGPS.[15] In this last report, the authors concluded that the *LMNA* truncation is a salvage alteration modifying the clinical picture from RD to HGPS by preventing farnesylation of the accumulated prelamin A or by reducing the amounts of the accumulated prelamin A. This second hypothesis is more probable from our point of view, since no truncated lamin A isoform was visible on the western blot. In all cases, farnesylated prelamin A accumulated while mature lamin A was either absent[15] or reduced.[14] Finally, 5 patients carrying compound heterozygous nonsense and missense *ZMPSTE24* mutations, have been described as being affected with MADB.[9,32-34] These *ZMPSTE24* mutations result in the presence of traces of prelamin A but also to mature lamin A[33] due to partial residual ZMPSTE24 activity.[9,32,33]

All these reports strongly suggest a link between the phenotype severity, prelamin A accumulation levels and ZMPSTE24 residual activity. Complete prelamin A accumulation with null ZMPSTE24 enzyme activity can be correlated to the most severe progeroid

syndrome, RD; null ZMPSTE24 activity rescued by a heterozygous *LMNA* null mutation causes a severe, HGPS-like, MADB phenotype, whereas partial accumulation of prelamin A with reduced ZMPSTE24 enzyme activity is associated to milder MADB phenotypes

The patient reported here during the 30 year follow up developed a MADB phenotype associated with a congenital myopathy, further extending the spectrum of clinical features associated to *ZMPSTE24* mutations. Furthermore, our patient's MADB phenotype seems to recapitulate, to some extent, the main features of RD. Intrauterine growth retardation, tight skin and arthrogryposis at birth are classical features of RD. The disease evolved progressively and the whole clinical phenotype such as failure to thrive, mandible and clavicle hypoplasia, distal acro-osteolysis, scleroderma like skin with subcutaneous calcifications appeared during the 1st and 2nd decades followed by vascular complications including high blood pressure and atherosclerosis as observed in other MADB patients. To our knowledge, this is the first report describing congenital myopathy in a patient affected with MADB.

The relatively mild progeroid phenotype of our patient is well correlated with the western blot analyses which showed highly reduced expression of ZMPSTE24, with residual activity, since reduced levels of mature lamin A and partial prelamin A accumulation coexist in the patient's cells. In addition, according to the *in silico* studies which predicted two conformational states of the mutated ZMPSTE24, we can imagine that one part of the mutated ZMPSTE24 is correctly folded despite the presence of mutation and is still functional, allowing normal maturation of prelamin A, whereas the other part missing the second TM domain and sharing enzymatic site and ER signal in the ER lumen, is either degraded or unable to cleave prelamin A. The existence of both conformations could explain both the reduced level of ZMPSTE24 and the partial prelamin A maturation detected by western blot.

At the cellular level, the coexistence of both prelamin A and lamins A and C leads to reduced life span of the cells with major nuclear abnormalities.[10,35]

From a phenotypic point of view, our patient suffered from particular features of prognostic value including impressive subcutaneous and vascular calcifications. The unusual

paravertabral diffuse calcinosis led to spinal cord compression requiring surgery. Such calcifications have been reported in 3 *ZMPSTE24* related MADB cases, 2 of them requiring surgical removal,[9,36] but not in the 2 others.[33] Similarly, a homozygous *LMNA* mutation c.1718C>T leading to the missense substitution p.Ser573Leu has been reported to result in progeroid features associated with arthropathy and tendinous calcinosis[37] without any prelamin A accumulation. Also, renal artery calcifications and chronic kidney disease were responsible for pharmacoresistant high blood pressure as observed in *ZMPSTE24* related MADB.[32] The glomerular and tubular abnormalities observed in our patient argue for a multifactorial aetiology.

In addition to progeroid features, our patient developed a clear and proven myopathy. She showed evidence of skeletal muscle involvement including muscle weakness with scapular winging, myopathic EMG pattern and fibre type disproportion with a predominance of small type I fibres and early respiratory insufficiency. These finding were unusual in the context of a *ZMPSTE24* related progeroid syndrome. Skeletal muscle abnormalities, including muscle atrophy, first proximally (scapulae, buttocks) then distally in the limbs, are classical symptoms described in HGPS.[38] As the diminished joint mobility observed in HGPS patients does not appear to be due to tightening of the skin, one may hypothesize that it may be due to muscle sclerosis and tightness similarly to what is observed in myopathies. The emergence of *LMNA* gene mutations in HGPS patients prompted the examination of skeletal muscle leading to the description of the first cases with progeroid syndrome and confirmed early onset myopathy due to p.Ser143Phe *LMNA* substitution[39,40] or type A MAD due to p.Arg471Cys homozygous[41] or p.Arg527His / Val440Met compound heterozygous[42] *LMNA* mutation. Among the 30 previously reported *ZMPSTE24* mutated patients; none had obvious or proven skeletal muscle involvement. While in our patient the first symptoms linked to muscle involvement appeared at 2.5y, RD patients never reach this age and usually die in the first hours/days after birth. Interestingly, even if none of the 5 *ZMPSTE24* related MADB cases[32-34] showed such myopathic involvement, one of these cases (patient 1 in[33]) showed clear

skeletal muscle fatty infiltration in gluteal and thigh muscles similar to what is described in other muscle diseases. On the other hand, *Zmpste24* knockout mice[18,19] are normal at birth but show slightly variable phenotypes. Skeletal muscle involvement manifested mainly by abnormal gait and muscle weakness with either a normal histological aspect[19] or a significant increase in abnormal small round fibers.[18] The myopathic signs in our patient were similar to those observed in *Zmpste24* knockout mice. The etiopathogenic mechanism of skeletal muscle involvement in our patient remains to be determined. Unfortunately, muscle cells of the patient could not be explored but, even if we cannot rule out the possibility that muscle disease is linked to one or more modifier genes, we suppose that they may exhibit reduced lifespan due to prelamin A accumulation, as do fibroblasts. Further skeletal muscle explorations in patients affected with MADB due to ZMPSTE24 loss of function might help to clarify this issue.

ACKNOWLEDGMENTS

We wish to thank Jean-Paul Leroy for his help in the clinical investigation of the patient, Thomas Voit for critical reading and fruitful discussion and the Myocastor study group for its constant support.

This work was financially supported by the *Institut National de la Santé et de la Recherche Médicale* (INSERM); the *Université Pierre et Marie Curie Paris 06* (UPMC); the *Université de la Méditerranée*, the *Centre National de la Recherche Scientifique* (CNRS); the *Association Française contre les Myopathies* (#11057, #11034); the European Union Sixth (Euro-laminopathies #018690) and Seventh (Myoage #223576) Framework Programmes.

Conflict of Interest Statement: The authors declare no conflict of interest.

REFERENCES

1 Kilic F, Johnson DA, Sinensky M: Subcellular localization and partial purification of prelamin A endoprotease: an enzyme which catalyzes the conversion of farnesylated prelamin A to mature lamin A. *FEBS Lett* 1999; **450**: 61-65.

2 Leung GK, Schmidt WK, Bergo MO *et al*: Biochemical studies of Zmpste24-deficient mice. *J Biol Chem* 2001; **276**: 29051-29058.

3 Lutz RJ, Trujillo MA, Denham KS, Wenger L, Sinensky M: Nucleoplasmic localization of prelamin A: implications for prenylation-dependent lamin A assembly into the nuclear lamina. *Proc Natl Acad Sci U S A* 1992; **89**: 3000-3004.

4 Varela I, Pereira S, Ugalde AP *et al*: Combined treatment with statins and aminobisphosphonates extends longevity in a mouse model of human premature aging. *Nat Med* 2008; **14**: 767-772.

5 Sinensky M, Fantle K, Trujillo M, McLain T, Kupfer A, Dalton M: The processing pathway of prelamin A. *J Cell Sci* 1994; **107 (Pt 1)**: 61-67.

6 Corrigan DP, Kuszczak D, Rusinol AE *et al*: Prelamin A endoproteolytic processing in vitro by recombinant Zmpste24. *Biochem J* 2005; **387**: 129-138.

7 Broers J, Ramaekers F, Bonne G, Ben Yaou R, Hutchison C: The nuclear lamins: laminopathies and their role in premature ageing. *Physiological Reviews* 2006; **86**: 967-1008.

8 Worman HJ, Bonne G: "Laminopathies": a wide spectrum of human diseases. *Exp Cell Res* 2007; **313**: 2121-2133.

9 Agarwal AK, Fryns JP, Auchus RJ, Garg A: Zinc metalloproteinase, ZMPSTE24, is mutated in mandibuloacral dysplasia. *Hum Mol Genet* 2003; **12**: 1995-2001.

10 Navarro C, De Sandre-Giovannoli A, Bernard R *et al*: Lamin A and ZMPSTE24 (FACE-1) defects cause nuclear disorganisation and identify restrictive dermopathy as a lethal neonatal laminopathy. *Hum Mol Genet* 2004; **13**: 2493-2503.

11 Navarro CL, Cadinanos J, Sandre-Giovannoli AD *et al*: Loss of ZMPSTE24 (FACE-1) causes autosomal recessive restrictive dermopathy and accumulation of Lamin A precursors. *Hum Mol Genet* 2005; **14**: 1503-1513.

12 Witt DR, Hayden MR, Holbrook KA, Dale BA, Baldwin VJ, Taylor GP: Restrictive dermopathy: a newly recognized autosomal recessive skin dysplasia. *Am J Med Genet* 1986; **24**: 631-648.

13 Novelli G, Muchir A, Sangiuolo F *et al*: Mandibuloacral dysplasia is caused by a mutation in LMNA encoding lamins A/C. *Am J Hum Genet* 2002; **71**: 426-431.

14 Shackleton S, Smallwood DT, Clayton P *et al*: Compound heterozygous ZMPSTE24 mutations reduce prelamin A processing and result in a severe progeroid phenotype. *J Med Genet* 2005; **42**: e36.

15 Denecke J, Brune T, Feldhaus T *et al*: A homozygous ZMPSTE24 null mutation in combination with a heterozygous mutation in the LMNA gene causes Hutchinson-Gilford progeria syndrome (HGPS): insights into the pathophysiology of HGPS. *Hum Mutat* 2006; **27**: 524-531.

16 Sander CS, Salman N, van Geel M *et al*: A newly identified splice site mutation in ZMPSTE24 causes restrictive dermopathy in the Middle East. *Br J Dermatol* 2008; **159**: 961-967.

17 Smigiel R, Jakubiak A, Esteves-Vieira V *et al*: Novel frameshifting mutations of the ZMPSTE24 gene in two siblings affected with restrictive dermopathy and review of the mutations described in the literature. *Am J Med Genet A* 2010; **152A**: 447-452.

18 Pendas AM, Zhou Z, Cadinanos J *et al*: Defective prelamin A processing and muscular and adipocyte alterations in Zmpste24 metalloproteinase-deficient mice. *Nat Genet* 2002; **31**: 94-99.

19 Bergo MO, Gavino B, Ross J *et al*: Zmpste24 deficiency in mice causes spontaneous bone fractures, muscle weakness, and a prelamin A processing defect. *Proc Natl Acad Sci U S A* 2002; **99**: 13049-13054.

20 Fong LG, Frost D, Meta M *et al*: A protein farnesyltransferase inhibitor ameliorates disease in a mouse model of progeria. *Science* 2006; **311**: 1621-1623.

21 Ben Yaou R, Toutain A, Arimura T *et al*: Multitissular involvement in a family with LMNA and EMD mutations: Role of digenic mechanism? *Neurology* 2007; **68**: 1883-1894.

22 Muchir A, Medioni J, Laluc M *et al*: Nuclear envelope alterations in fibroblasts from patients with muscular dystrophy, cardiomyopathy, and partial lipodystrophy carrying lamin A/C gene mutations. *Muscle Nerve* 2004; **30**: 444-450.

23 Decary S, Mouly V, Hamida CB, Sautet A, Barbet JP, Butler-Browne GS: Replicative potential and telomere length in human skeletal muscle: implications for satellite cell-mediated gene therapy. *Hum Gene Ther* 1997; **8**: 1429-1438.

24 Thill M, Nguyen TD, Wehnert M *et al*: Restrictive dermopathy: a rare laminopathy. *Arch Gynecol Obstet* 2008; **278**: 201-208.

25 Moulson CL, Go G, Gardner JM *et al*: Homozygous and compound heterozygous mutations in ZMPSTE24 cause the laminopathy restrictive dermopathy. *J Invest Dermatol* 2005; **125**: 913-919.

26 Morais P, Magina S, Ribeiro Mdo C *et al*: Restrictive dermopathy--a lethal congenital laminopathy. Case report and review of the literature. *Eur J Pediatr* 2009; **168**: 1007-1012.

27 Kariminejad A, Goodarzi P, Thanh Huong le T, Wehnert MS: Restrictive dermopathy. Molecular diagnosis of restrictive dermopathy in a stillborn fetus from a consanguineous Iranian family. *Saudi Med J* 2009; **30**: 150-153.

28 Chen M, Kuo HH, Huang YC *et al*: A case of restrictive dermopathy with complete chorioamniotic membrane separation caused by a novel homozygous nonsense mutation in the ZMPSTE24 gene. *Am J Med Genet A* 2009; **149A**: 1550-1554.

29 Jagadeesh S, Bhat L, Suresh I, Muralidhar SL: Prenatal diagnosis of restrictive dermopathy. *Indian Pediatr* 2009; **46**: 349-351.

30 Li C: Homozygosity for the common mutation c.1085dupT in the ZMPSTE24 gene in a Mennonite baby with restrictive dermopathy and placenta abruption. *Am J Med Genet A* 2010; **152A**: 262-263.

31 Fong LG, Ng JK, Meta M *et al*: Heterozygosity for Lmna deficiency eliminates the progeria-like phenotypes in Zmpste24-deficient mice. *Proc Natl Acad Sci U S A* 2004; **101**: 18111-18116.

32 Agarwal AK, Zhou XJ, Hall RK *et al*: Focal segmental glomerulosclerosis in patients with mandibuloacral dysplasia owing to ZMPSTE24 deficiency. *J Investig Med* 2006; **54**: 208-213.

33 Miyoshi Y, Akagi M, Agarwal AK *et al*: Severe mandibuloacral dysplasia caused by novel compound heterozygous ZMPSTE24 mutations in two Japanese siblings. *Clin Genet* 2008; **73**: 535-544.

34 Cunningham VJ, D'Apice MR, Licata N, Novelli G, Cundy T: Skeletal phenotype of mandibuloacral dysplasia associated with mutations in ZMPSTE24. *Bone* 2010.

35 Goldman RD, Shumaker DK, Erdos MR *et al*: Accumulation of mutant lamin A causes progressive changes in nuclear architecture in Hutchinson-Gilford progeria syndrome. *Proc Natl Acad Sci U S A* 2004; **101**: 8963-8968.

36 Agarwal AK, Kazachkova I, Ten S, Garg A: Severe mandibuloacral dysplasia-associated lipodystrophy and progeria in a young girl with a novel homozygous Arg527Cys LMNA mutation. *J Clin Endocrinol Metab* 2008; **93**: 4617-4623.

37 Van Esch H, Agarwal AK, Debeer P, Fryns JP, Garg A: A homozygous mutation in the lamin A/C gene associated with a novel syndrome of arthropathy, tendinous calcinosis, and progeroid features. *J Clin Endocrinol Metab* 2006; **91**: 517-521.

38 Hennekam RC: Hutchinson-Gilford progeria syndrome: review of the phenotype. *Am J Med Genet A* 2006; **140**: 2603-2624.

39 Kirschner J, Brune T, Wehnert M *et al*: p.S143F mutation in lamin A/C: a new phenotype combining myopathy and progeria. *Ann Neurol* 2005; **57**: 148-151.

40 Madej-Pilarczyk A, Kmiec T, Fidzianska A *et al*: Progeria caused by a rare LMNA mutation p.S143F associated with mild myopathy and atrial fibrillation. *Eur J Paediatr Neurol* 2008; **12**: 427-430.

41 Zirn B, Kress W, Grimm T *et al*: Association of homozygous LMNA mutation R471C with new phenotype: mandibuloacral dysplasia, progeria, and rigid spine muscular dystrophy. *Am J Med Genet A* 2008; **146A**: 1049-1054.

42 Lombardi F, Gullotta F, Columbaro M *et al*: Compound heterozygosity for mutations in LMNA in a patient with a myopathic and lipodystrophic mandibuloacral dysplasia type A phenotype. *J Clin Endocrinol Metab* 2007; **92**: 4467-4471..

Titles and legends to figures

Figure 1. Patient clinical features. ***a.*** Photographs of the patient at different ages showing general habitus, mandibular hypoplasia (a_{3-6}, arrows), abdominal skin papules with dry skin (a_2), pronounced abdominal (a_3) and hand (a_6) veins and alopecia (a_6). ***b.*** Chest X-ray showing (arrows) dysplastic clavicles (b_{1-4}), right clavicle (b_{5-6}) and lower femur extremity (b_7) fractures as well as subcutaneous cervical and dorsal calcifications (b_8). ***c.*** Skull, hand and chest X-ray showing mandible hypoplasia (c_1), delayed skill ossification, cranial sutures closing and teeth development (c_{2-4}), hands subcutaneous calcifications of the inter-phalangian joints with distal fingers acro-osteolysis (c_{5-6}), enlarged metaphysis with slender diaphysis of long bones (c_5) and diffuse subcutaneous cervical and dorsal calcifications (c_{8-9}). ***d.*** Deltoid muscle biopsy (d_1) with haematoxylin-Eosin (HE), modified Gomori Trichrome (GT) and ATPase pH 4.6 and 9.4 stainings showing fibre size variation, predominance of small type I fibres. CT scan coupled with angiography showing (arrows) bilateral calcifications at the renal arteries origin (d_2) and atheromatous aortic infiltration (d_3).

Figure 2. Characterisation of the *ZMPSTE24* mutation. ***a.*** Genomic DNA sequences of patient and control showing the homozygous transition c.281T>C, p.Leu94Pro in *ZMPSTE24* exon 3 gene. ***b.*** Analysis of the segregation of the *ZMPSTE24* variant within the family. Circles indicate females, squares indicate males, clear symbols indicate healthy subjects, black symbols indicate patients, “m” indicates the mutated allele in each subject in the homozygous state (m/m) or the heterozygous state (m/+). The mutation creates a new *Bsl*I site in a 235-bp PCR fragment of exon 3. *Bsl*I digestion identifies two alleles: an uncut fragment indicates the wild-type allele; two additional bands indicate the mutated allele. ***c.*** Partial amino acid sequence alignment of ZMPSTE24 from various species. The conservation of Leu94 is highlighted within the red box. ***d.*** *In silico* predictions of the possible consequence of *ZMPSTE24* mutation. TMHMM and TMpred programs, using either normal or mutated ZMPSTE24 protein sequences as matrix, indicated two possible conformation models. ***e.***

Western blot analysis of ZMPSTE24 and A-type lamins at passage P2. The reduction of ZMPSTE24 in patient's cultured skin fibroblasts is associated with accumulation of prelamin A.

Figure 3. Immuno-fluorescence analysis of the patient's fibroblasts. Patient fibroblasts grow as clusters and exhibit highly variable size with a majority of the cells being larger than control cells. Patient cells exhibited major nuclear shape defects, i.e. lobulations, herniations, with lamins A/C and emerin still localised at the nuclear rim. Prelamin A was present in all patient fibroblasts. Analyses were performed at passage P2. Scale bar represents 20 µm.

Figure 4. *In vitro* Life span of Fibroblasts. Cell populations were serially passaged in growth medium until the cells ceased to divide. At each passage the mean number of population doublings was determined by counting the cells. Patient fibroblasts showed a dramatically decreased replicative potential compared to cell isolated from a health control.


a1
3.5mo


a2
12mo

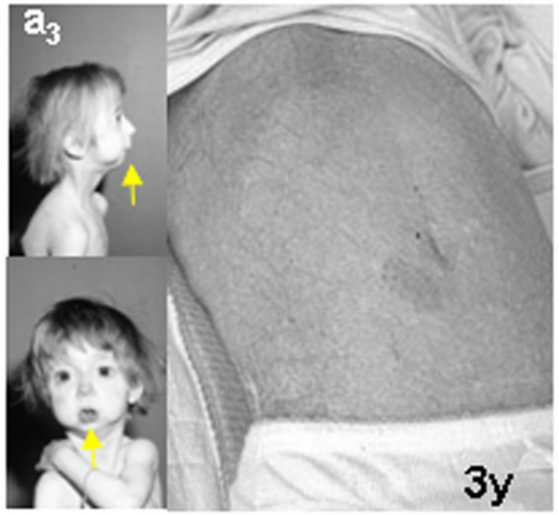
a3
3y

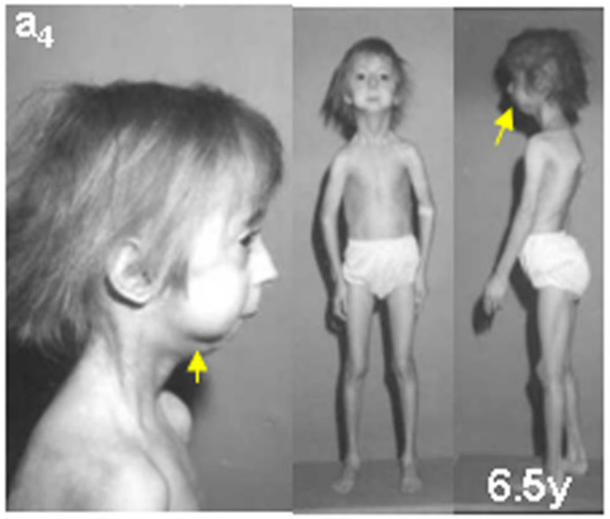
a4
6.5y

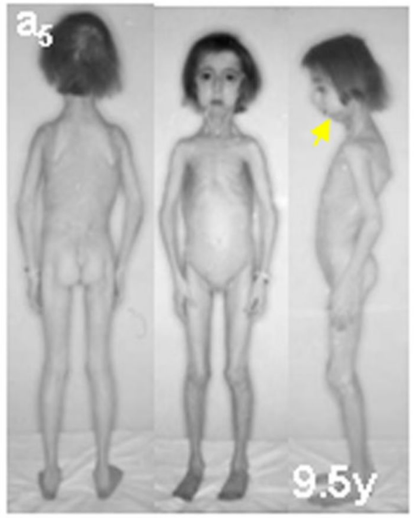
a5
9.5y

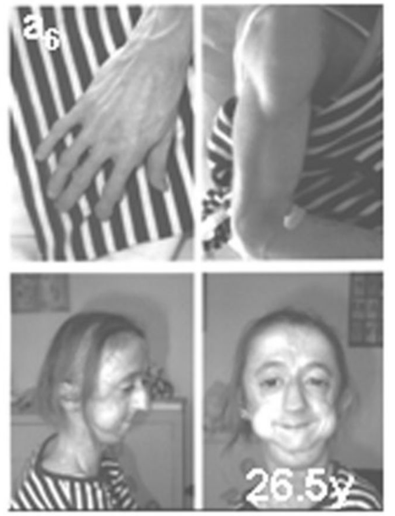
a6
26.5y

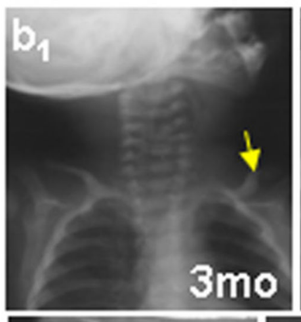
b1
3mo

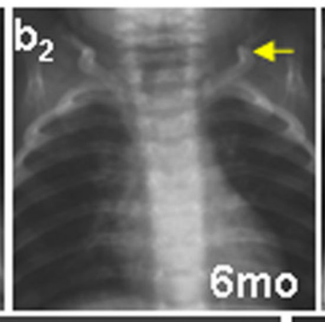
b2
6mo

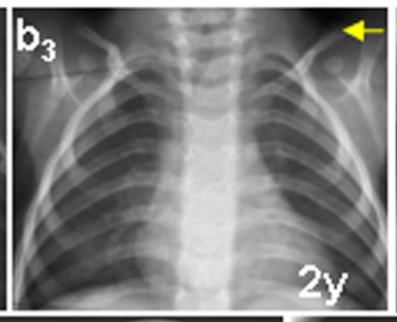
b3
2y

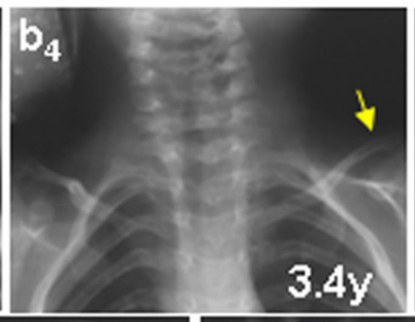
b4
3.4y

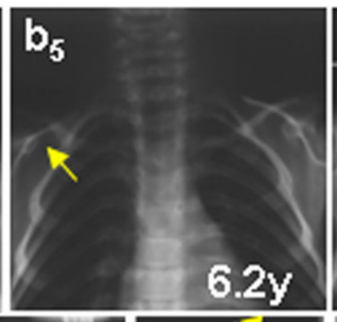
b5
6.2y

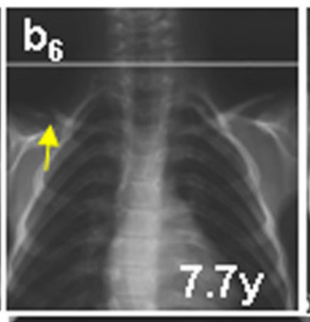
b6
7.7y

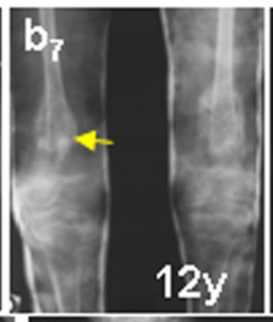
b7
12y

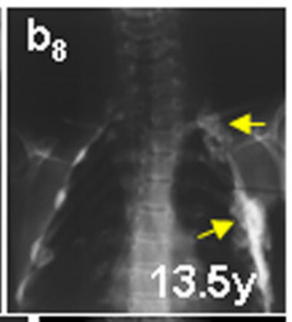
b8
13.5y

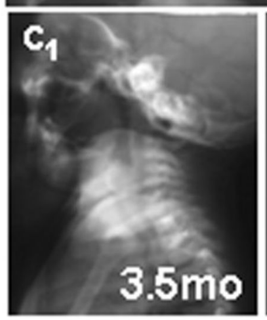
c1
3.5mo

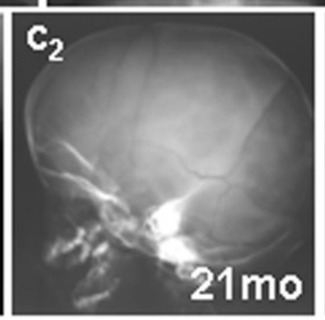
c2
21mo

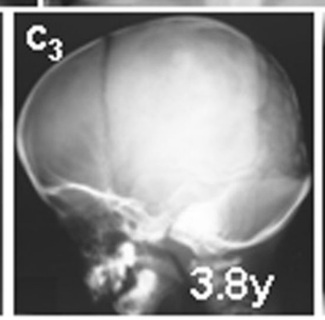
c3
3.8y

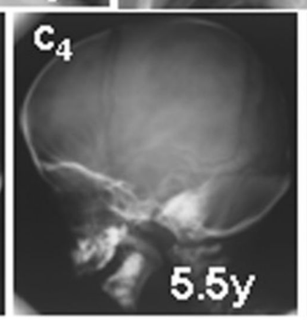
c4
5.5y


c5
11.5y


c6
13.25y

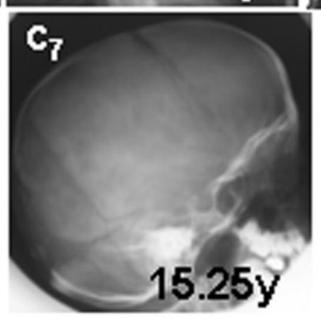
c7
15.25y


c8
14.75y


c9
22.5y

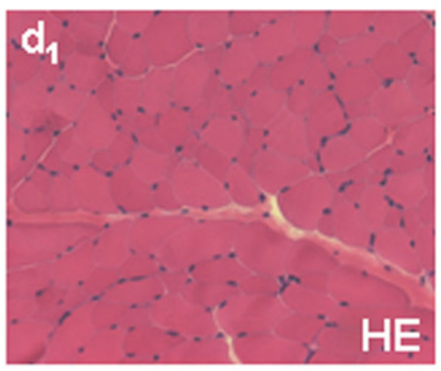
d1
HE

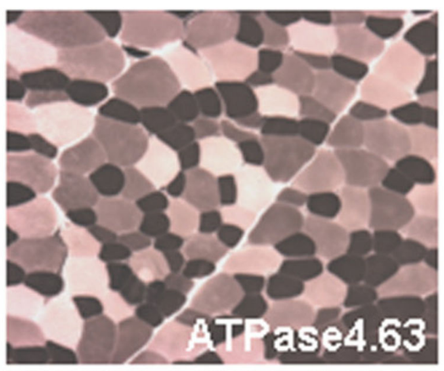
ATPase4.63

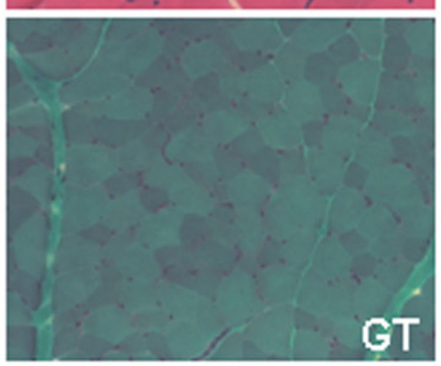
GT

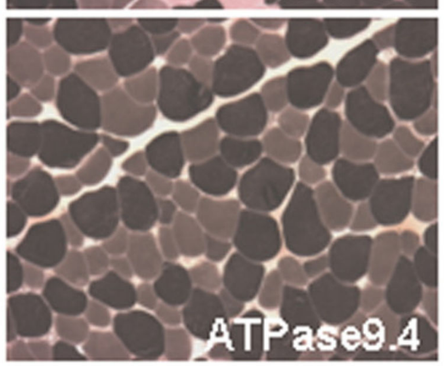
ATPase9.4


d2

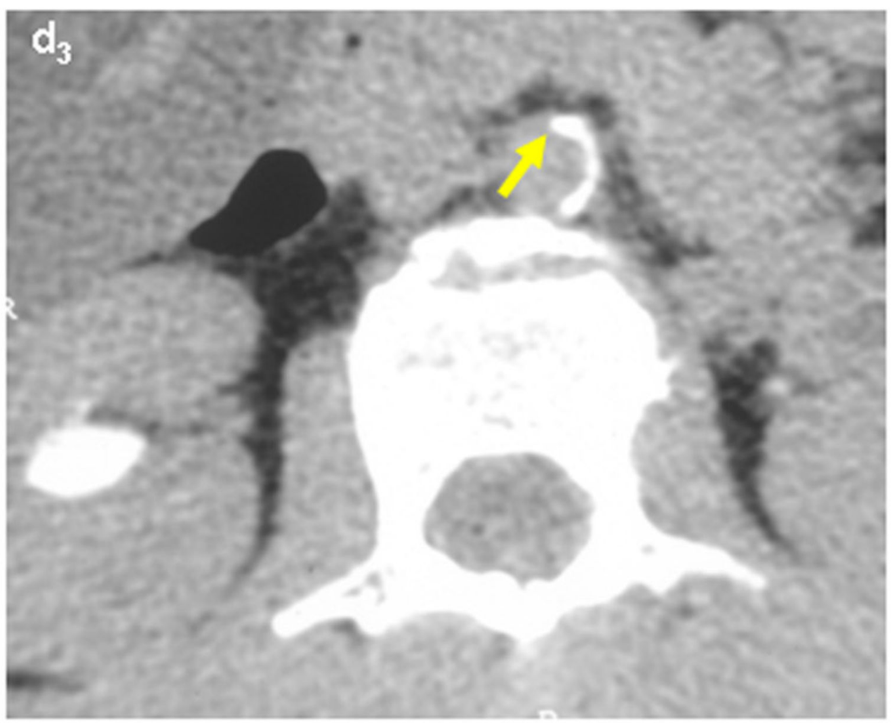
d3

a

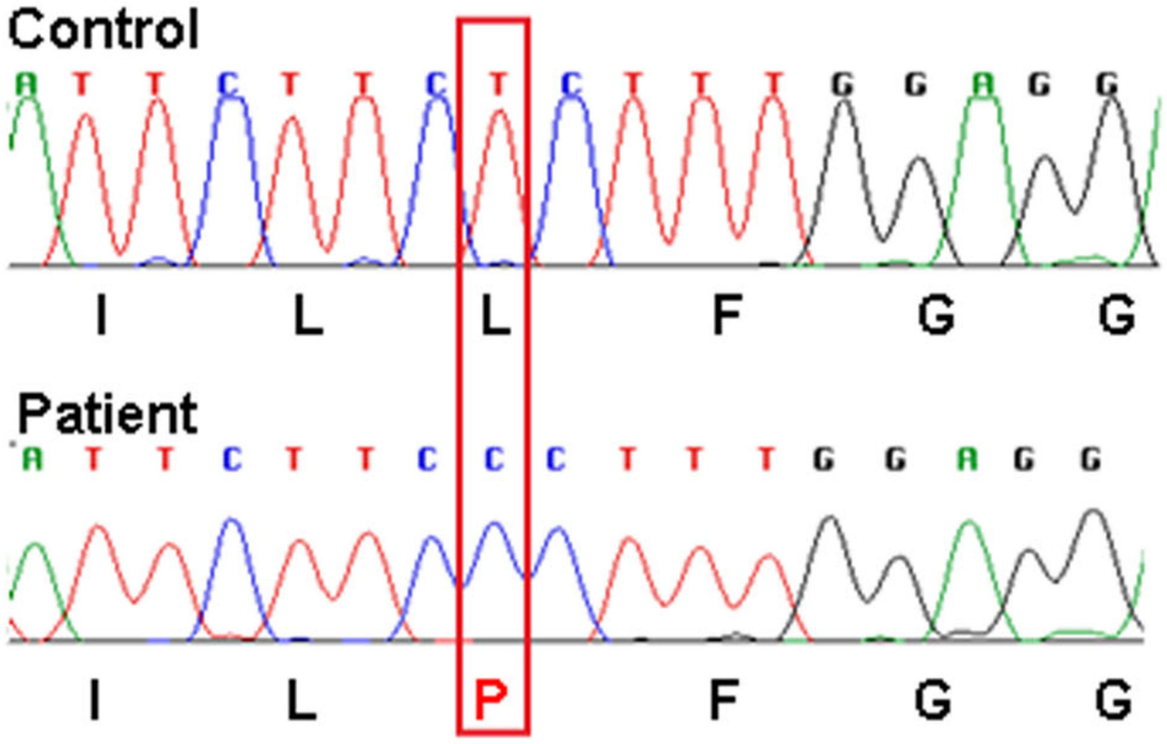

b

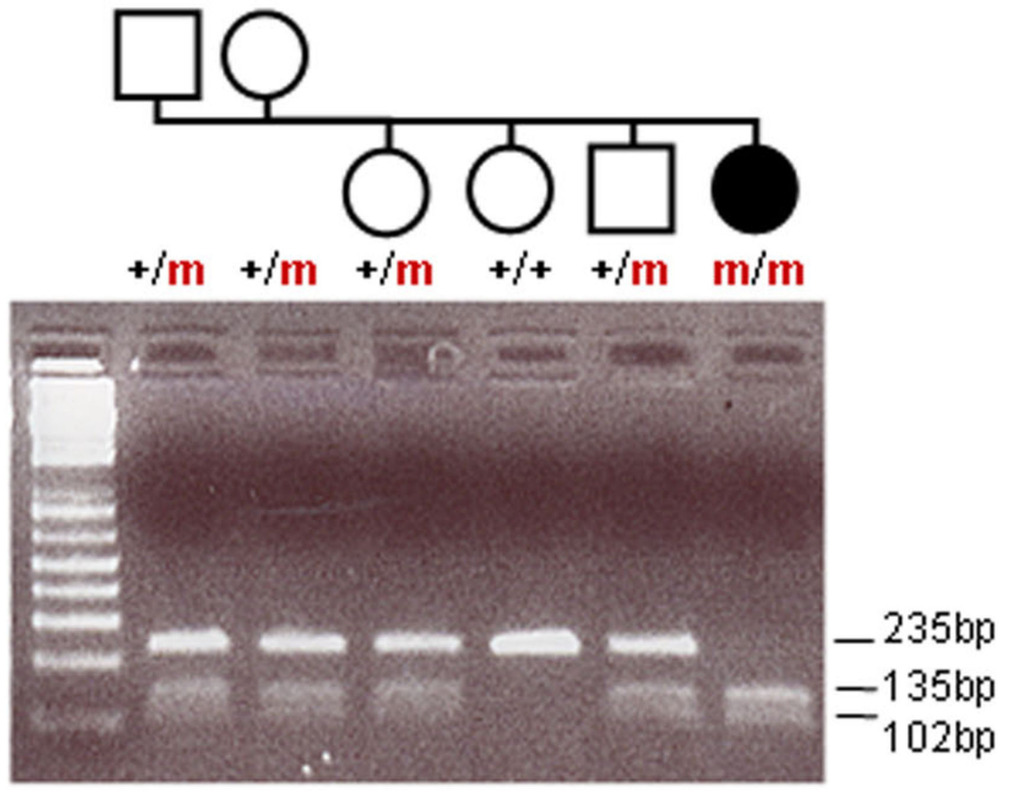

c

d

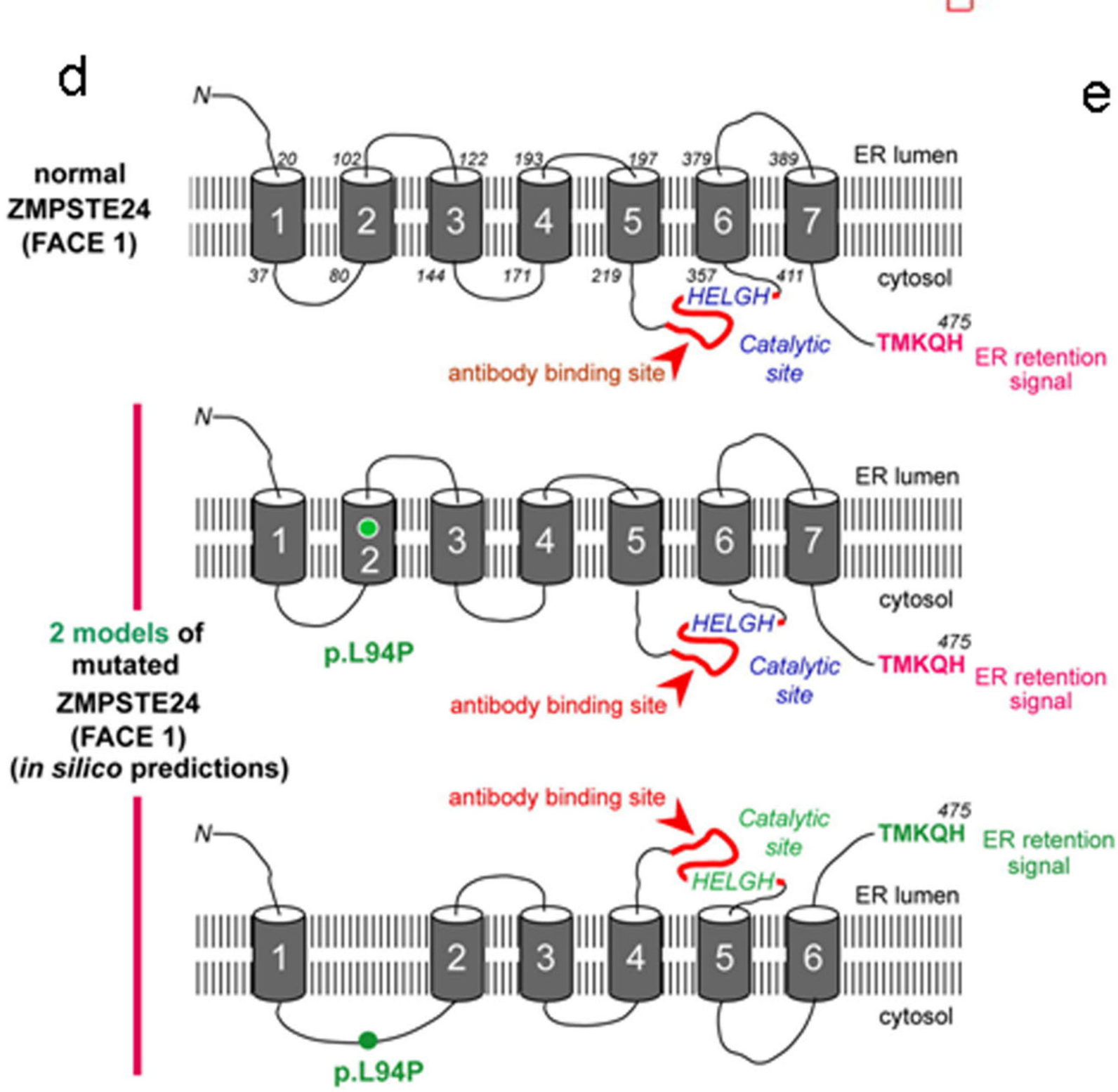

e

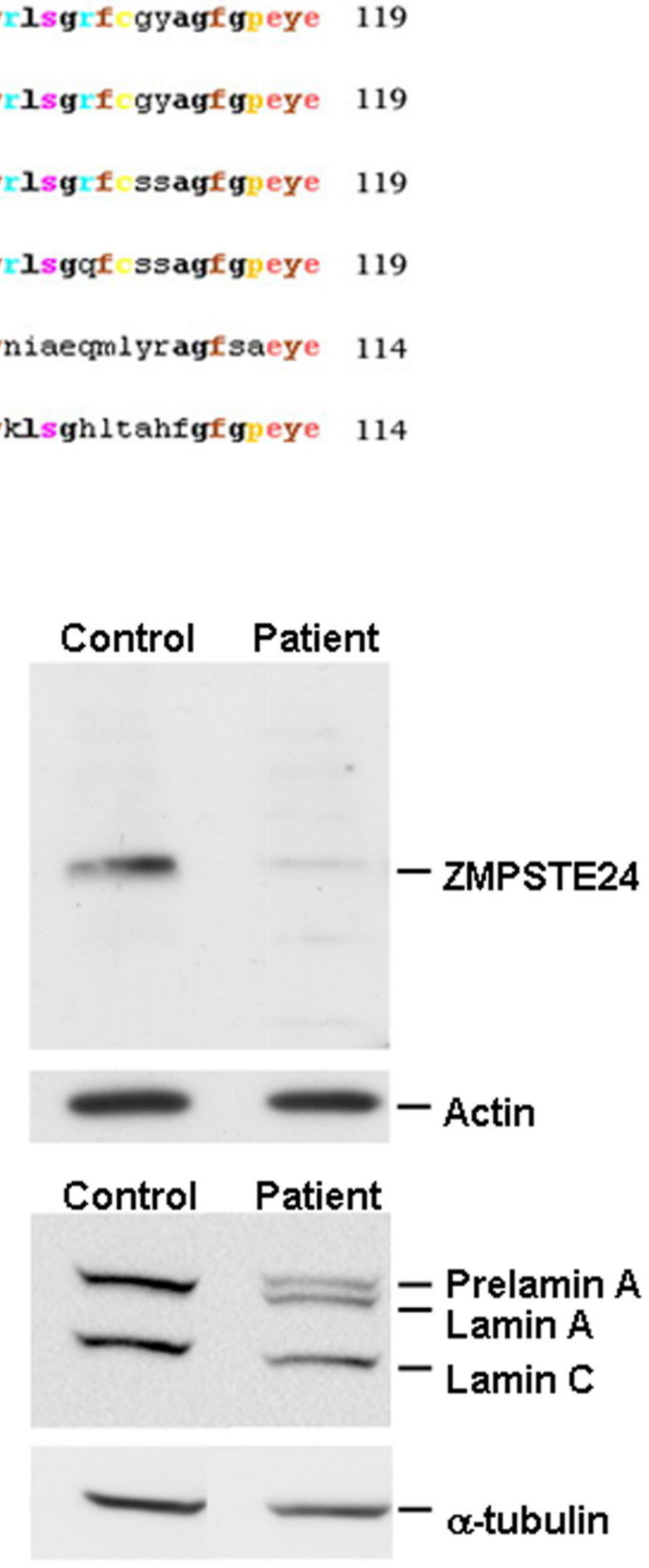

Figure 2

Figure 3

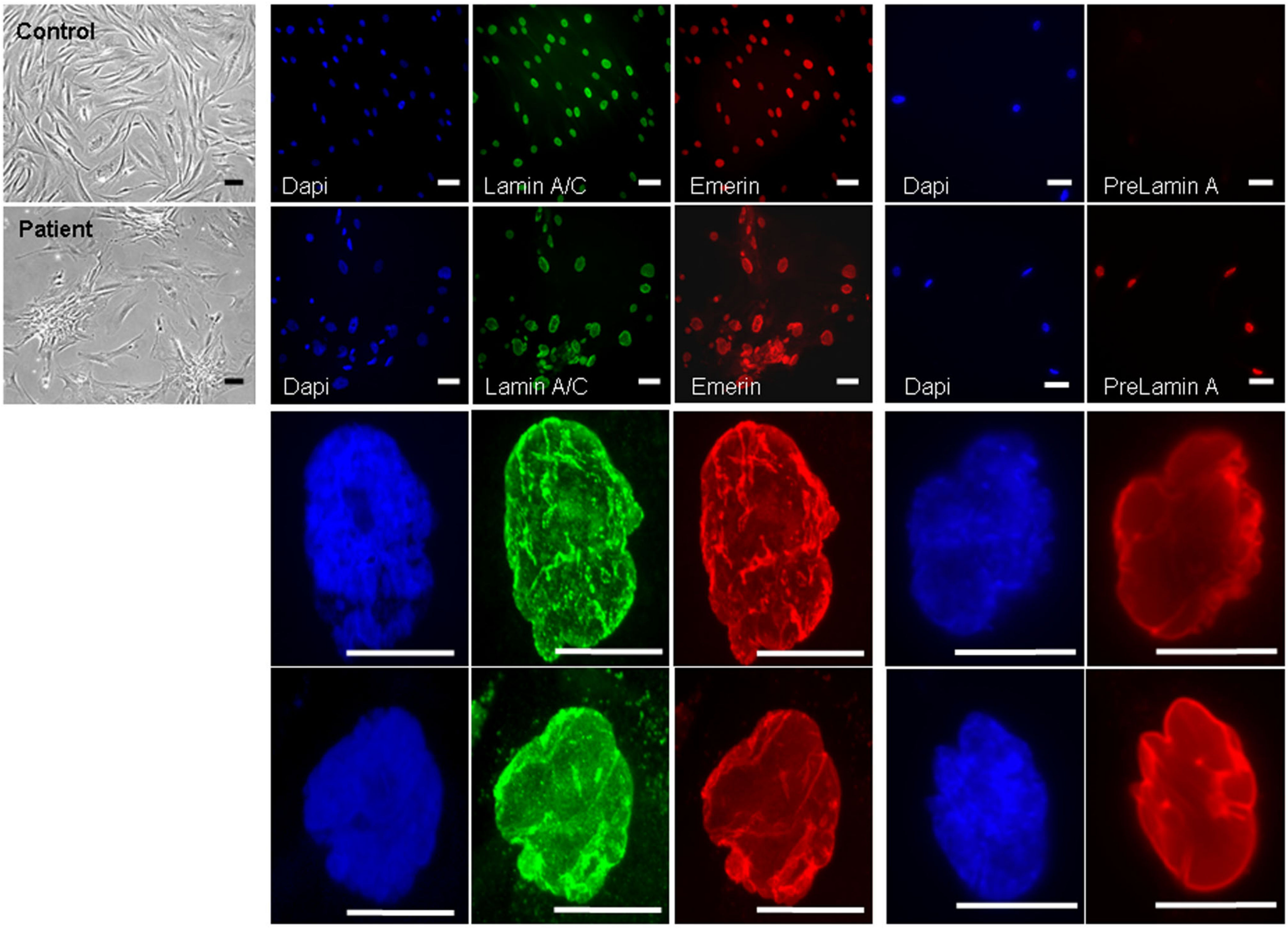
Control
Patient
Dapi
Lamin A/C
Emerin
Dapi
PreLamin A
Dapi
Lamin A/C
Emerin
Dapi
PreLamin A

Figure 4

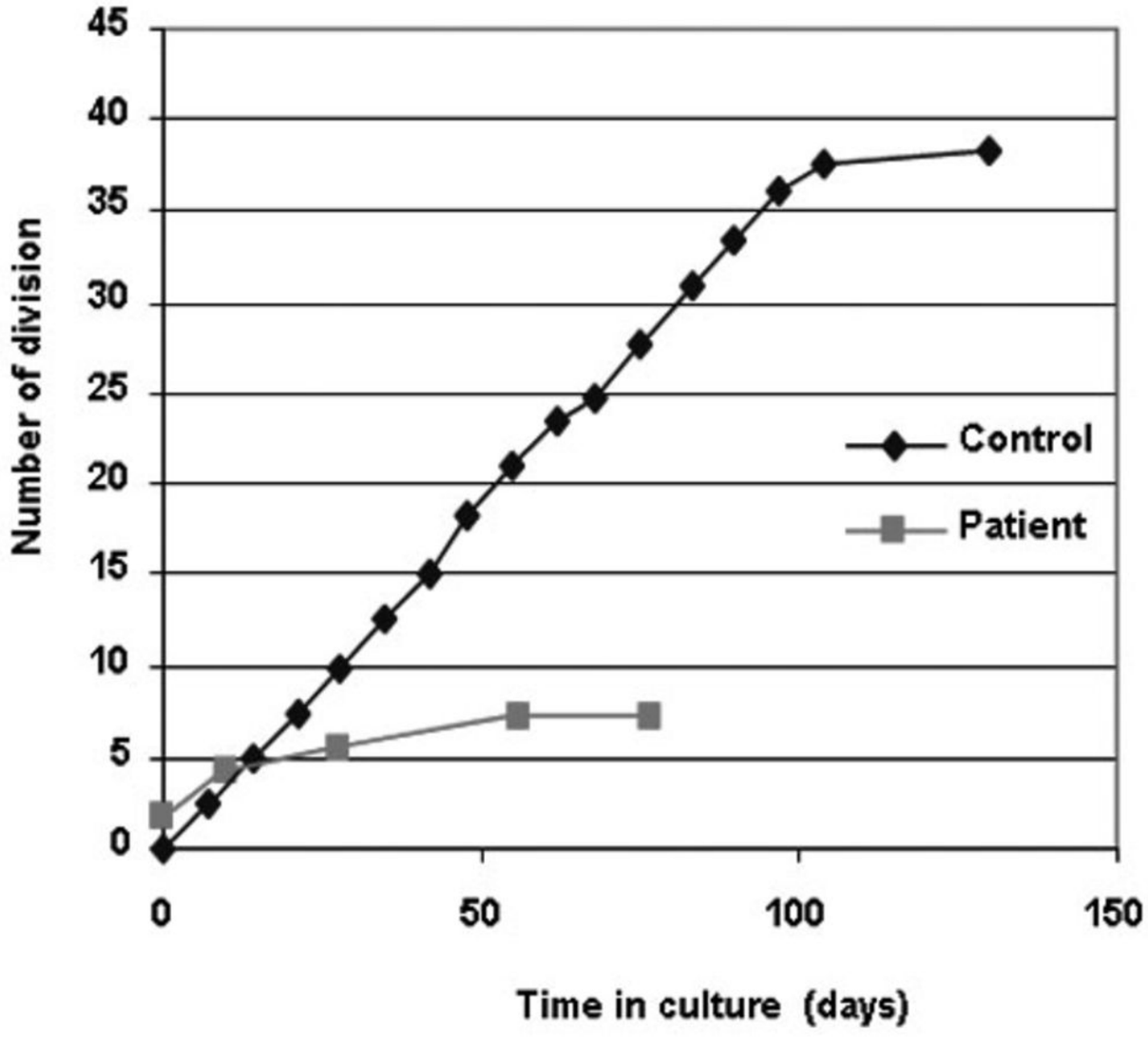
45
40
35
30
25
20
15
10
5
0
0
50
100
150
Number of division
Time in culture (days)
Control
Patient